Chapter 4

Optimal Coordination of PV smart inverter and traditional Volt-VAR control devices for energy cost savings and voltage regulation

4.1 Introduction

Traditional Volt-VAR control (VVC) devices such as on-load tap changers (OLTC), voltage regulators (VRs) and shunt capacitor banks (SCBs) may not be capable to handle the sudden voltage violations because of slow response and large delay time [51] [52]. The voltage fluctuations may result from various disturbances such as intermittence in power output from distributed energy sources (DERs) such as photovoltaic (PV) and wind generation, change in network configuration and load demand (especially in case of the flexible loads). Hence, there is a need of fast acting voltage regulation device such as smart inverter along with traditional VVC devices to encounter these issues. However, without proper coordination, these devices may cause a detrimental impact on distribution operations and network assets.

In order to resolve aforementioned issues, a hierarchical coordinated volt-VAR optimization (VVO) methodology has been introduced in this chapter. In the proposed methodology, centralised as well as local control algorithm has been considered. The VVO objective of present chapter is to minimize the total operating cost considering

conservation voltage reduction (CVR) and voltage deviation at all nodes simultaneously. Besides, Impact of battery energy storage (BES) on total operating cost, voltage deviation and CVR has been examined.

The main contributions of this chapter are as follows

- A hierarchical coordinated volt-VAR optimization (VVO) methodology has been proposed considering traditional and advanced VVC devices.
- A multi-objective problem has been formulated considering total operating cost and voltage deviation
- Impact of BES on total operating cost, voltage deviation and CVR has been studied
- Utilizing the $\varepsilon-$constraint method to obtain set of non-inferior solutions and fuzzy decision-making method to determine the best compromise solution among the set of non-inferior solutions.
- Impact of forecast errors of PV generation and load demand has also been examined on proposed methodology

4.2 Proposed hierarchical coordinated VVO methodology

In this study, VVC devices are categorised as slow acting VVC devices and fast acting VVC devices. The OLTC, VRs, and SCBs can be considered as slow acting VVC devices because of their slow response and large delay time. Whereas smart inverter can be considered as fast acting VVC devices. Under normal conditions slow acting VVC devices can capable to maintain the voltage with in permissible limits. However, these devices fail to handle abnormal condition such as sudden change in PV generation output and load demand. Fast acting VVC devices could be a better choice under such conditions. However, without proper coordination of these devices lead to negative impact on distribution operations and network assets. In order resolve this issue, a hierarchical coordinated volt-VAR optimization (VVO) methodology has been employed, which comprises of centralised as well as local control algorithms as illustrated in Fig. 4.1.

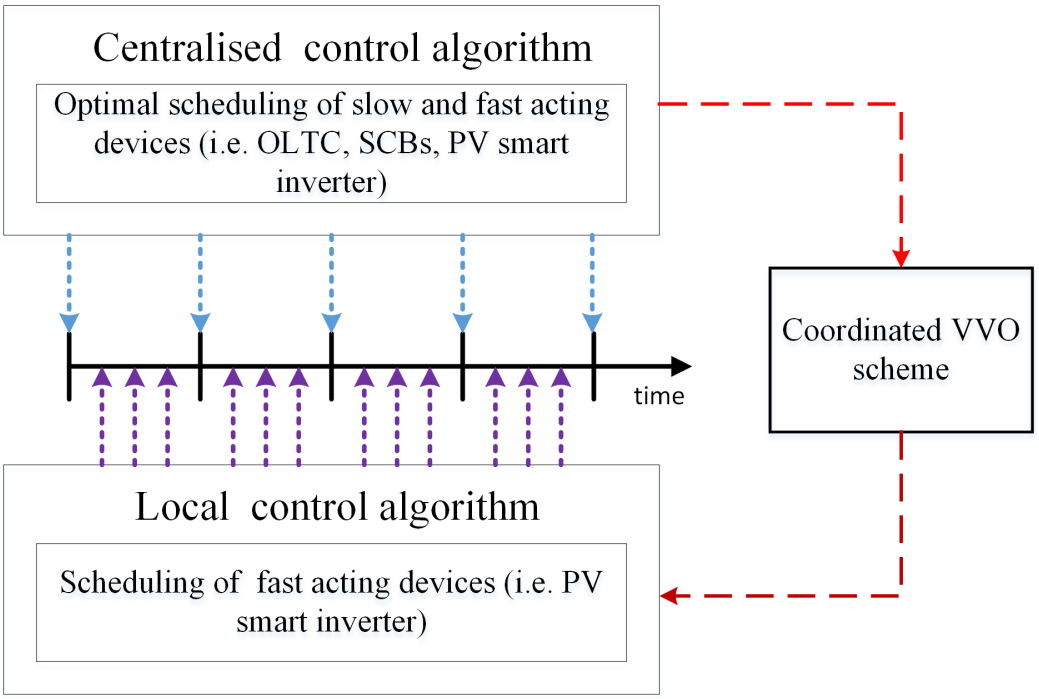

Figure 4.1: Schematic of proposed hierarchical coordinated VVO methodology

In centralised control algorithm, optimal scheduling of the slow acting devices (i.e. OLTC and SCBs) as well as fast acting devices (i.e. PV smart inverter) have been determined at hourly basis. Whereas, scheduling of fast acting devices has been determined at intra- hourly basis in local control algorithm. For coordination purposes, the local control algorithm receives the obtained PV reactive power from centralised control algorithm. Further, change of PV reactive power scheduling has been done based on volt-VAR characteristics of smart inverter. The detailed explanation of the proposed hierarchical coordinated VVO methodology has been given in the section 4.4.

4.3 Problem formulation

Power system utilities are more concerned towards the loss minimization, volt-VAR control, voltage deviation minimization, energy savings and assure the good power quality service to the consumers. In order to accomplish these issue, centralised control and operation of distribution networks assets such as OLTC, VRs, SCBs, BES and reactive power compensators need to operate in efficient and optimal manner. Further, local control is much needed to avoid the voltage limits violations during sudden variation in PV generation, network configuration and load demand. Considering these aspects, the present

problem has been formulated such that it covers the centralised as well as a local control with the multi-objective energy cost savings via CVR and voltage regulation. The objective functions of this problem have been delineated as under

4.3.1 Objective functions

(i) *Minimization of total operating cost (OF_i)*: Minimization of total operating cost can be viewed as maximization of cost of energy savings. The total operating cost comprises of cost of energy purchased from grid as well as PVs (it can be refereed as a cost of energy demand) and operating cost of OLTC, SCBs, SI and BES as given in equation (4.1)

$$OF_1 = \sum_{t=1}^{T} \left(\begin{array}{l} \pi_{grid}^{p,t}.P_{grid}^{t} + \pi_{grid}^{q}.Q_{grid}^{t} + \sum\limits_{i\in\Omega_{pv}} \pi_{pv}^{p,t}.P_{i,pv}^{t} + \sum\limits_{i\in\Omega_{pv}} \pi_{pv}^{q,t}.Q_{i,pv}^{t} \\ + \sum\limits_{i\in\Omega_{bes}} \pi_2.P_{i,BES}^{dis,t} + \pi^{tap}.\left|tap^{t} - tap^{t-1}\right| + \sum\limits_{i\in\Omega_{cap}} \pi^{cap}.\left|st_i^{t} - st_i^{t-1}\right| \end{array} \right) \quad (4.1)$$

The first term of equation (4.1) represents the cost of active power purchased from the grid that includes the cost of active power loss ($\pi_{grid}^{p,t}.\sum\limits_{i=1}^{nd} P_{i,loss}^{t}$) as well as cost of battery charging ($\pi_{grid}^{p,t}.\sum\limits_{i\in\Omega_{bes}} P_{i,BES}^{ch,t}$) . Similarly, second term represents the cost of reactive power purchased from the grid. The third and fourth term represents the cost of active and reactive power purchased from the PV respectively. The fifth term represents variable operating & maintenance cost of BESS respectively. The sixth and seventh term represents switching operating cost of OLTC and SCBs. Here, the reactive power purchased from the PV is equivalent to cost of additional active power loss of PV smart inverter ($P_{loss,pv}^{inv}$) [143]. Normally, this ($P_{loss,pv}^{inv}$) is compensated by PV during the daytime and by grid (P_{grid}) in the dawn and at night. However, in this study, the $\Delta P_{loss,pv}^{inv}$ has been compensated by taking more power from the grid since PV generation has been assumed less than the total load demand. Therefore, the cost of reactive power supplied by PV inverter is given by equation (4.2).

$$\pi_{pv}^{q,t}.Q_{i,pv}^{t} = \pi_{grid}^{p,t}.\Delta P_{i,loss}^{inv,t} \quad (4.2)$$

Here, inverter power loss can be calculated as

$$P_{loss}^{inv} = c_s + c_v S_{inv} + c_R S_{pv}^{2} \quad (4.3)$$

The additional active power loss due to the injection of reactive power is given by

equation (4.4)

$$\Delta P_{i,pv}^{loss,t} = \begin{cases} c_v\left(S_{i,pv}^t - P_{i,pv}^t\right) + c_R\left(\left(S_{i,pv}^t\right)^2 - \left(P_{i,pv}^t\right)^2\right) & P_{i,pv}^t \neq 0 \\ c_s + c_v Q_{i,pv}^t + c_R\left(Q_{i,pv}^t\right)^2 & P_{i,pv}^t = 0 \end{cases} \tag{4.4}$$

(ii)*Minimization of total voltage deviation (OF_2)*: Sum of voltage deviation of the all the buses over specific period T is given as in equation (4.5)

$$OF_2 = \frac{\sum_{t=1}^{T} V_{dv}^t}{T} \tag{4.5}$$

Where, $V_{dv}^t = \sum_{i=1}^{Nbus} \left|\frac{V^{spec.} - V_i^t}{V^{spec.}}\right|$

Here equation (4.1) and (4.5) treated as two objectives to be minimized subjected operational and system constraints

4.3.2 Operational and system constraints

- Active and reactive power balance constraints

$$P_{grid}^t - \sum_{i=1}^{nd} P_{i,loss}^t - \sum_{i=1}^{nd} P_{i,cons}^t + \sum_{i\in\Omega_{pv}} P_{i,pv}^t - \sum_{i\in\Omega_{bes}} P_{i,BES}^{ch,t} + \sum_{i\in\Omega_{bes}} P_{i,BES}^{dis,t} = 0 \tag{4.6}$$

$$Q_{grid}^t - \sum_{i=1}^{nd} Q_{i,loss}^t - \sum_{i=1}^{nd} Q_{i,cons}^t + \sum_{i\in\Omega_{cap}} Q_{i,cap}^t + \sum_{i\in\Omega_{pv}} Q_{i,pv}^t = 0 \tag{4.7}$$

here $P_{i,loss}^t = |I_i^t| \times R_i; Q_{i,loss}^t = |I_i^t| \times X_i$; where $|I_i^t| = \left(\frac{P_i^t + Q_i^t}{V_i^t}\right)^*$

- System voltage magnitude limits

$$V^{\min} \leq V_i^t \leq V^{\max} \tag{4.8}$$

- Tap settings of OLTC transformer

$$a^t = 1 + tap^t \frac{\Delta tap_{step}}{100} \tag{4.9}$$

here, $tap^t \in \left\{tap^{\min}, ..., -1, 0, 1, ...tap^{\max}\right\}$

- Limits of taps operation of OLTC transformer

$$\sum_{t=1}^{24} \left|tap^t - tap^{(t-1)}\right| \leq MAO^{tr} \tag{4.10}$$

- Switched capacitor banks (SCBs)

$$Q_{i,cap}^{t} = st_{i}^{t}\Delta q_{i}^{cap}; i \in \Omega_{cap} \tag{4.11}$$

Where, $st_{i}^{t} \in \{0, 1, ...st_{i}^{\max}\}$

- Limits of switching operation of SCBs

$$\sum_{t=1}^{24} \left| st_{i}^{t} - st_{i}^{(t-1)} \right| \leq MAO^{cap} \tag{4.12}$$

- Reactive power limit of smart inverter

$$Q_{i,pv}^{t} = \sqrt{\left(S_{i,pv}^{\max}\right)^{2} - \left(P_{i,pv}^{t}\right)^{2}}; i \in \Omega_{pv} \tag{4.13}$$

$$-Q_{i,pv}^{\max} \leq Q_{i,pv}^{t} \leq Q_{i,pv}^{\max} \tag{4.14}$$

- Power limits of Battery energy storage

$$0 \leq P_{i,BES}^{ch/dis,t} \leq P_{BES}^{rated}; i \in \Omega_{bes} \tag{4.15}$$

SOC limits of Battery energy storage

$$SOC_{BES}^{\min} \leq SOC_{i,BES}^{t} \leq SOC_{BES}^{\max}; i \in \Omega_{bes} \tag{4.16}$$

$$SOC_{i}^{t} = SOC_{i}^{t-1} + \left(\delta_{i}^{ch,t}.\eta^{ch}.P_{i,BES}^{ch,t} + \frac{\delta_{i}^{dis,t}.P_{i,BES}^{dis,t}}{\eta_{i}^{dis}} \right) \frac{\Delta t}{E_{i,BES}^{rated}} \tag{4.17}$$

$$\delta_{i}^{ch,t} + \delta_{i}^{dis,t} \leq 1; \delta_{i}^{ch,t}, \delta_{i}^{dis,t} \in \{0, 1\} \tag{4.18}$$

4.3.3 Voltage dependent Load models (VDLM)

Generally, utility takes the responsibility for delivering power to every consumer by appropriate voltage level. In medium/low voltage distribution network, most of the loads exhibit the voltage dependant behaviour [120]. These loads are highly dependent on the voltage magnitude. There are two VDLMs namely exponential and polynomial loads. In this chapter, exponential load voltage dependents have been chosen to represent the load-to-voltage sensitivities in this study.

$$P_{i,cons}^{t} = P_{i,cons}^{nom,t} \left(\frac{V_{i}^{t}}{V^{nom}} \right)^{k_{i}^{q}} \tag{4.19}$$

$$Q_{i,cons}^{t} = Q_{i,cons}^{nom,t} \left(\frac{V_{i}^{t}}{V^{nom}} \right)^{k_{i}^{q}} \tag{4.20}$$

4.3.4 Conservation voltage reduction (CVR)

CVR is a viable technique employed by utilities for peak demand reduction and energy savings. The main principle of CVR is to achieve energy savings by decreasing the voltage level in distribution feeder, which ensuring that the nodal voltages within acceptable voltage limits and without affects the performance of voltage sensitive customers [53]. According to American National Standards Institute (ANSI), the allowable range of voltages at the distribution transformer secondary terminals can be set as $\pm 5\%$ of the nominal value. In this chapter, CVR operation has been performed by coordinated operation of PV smart inverter with traditional Volt $-$ VAR control devices.

4.4 Implementation of proposed hierarchical coordinated control scheme

As said earlier in section 4.2, the optimal settings of traditional VVC devices and smart inverter of PV systems have been determined in centralised control algorithm on hourly basis. The setting obtained by centralised control algorithm, distribution system could operate optimally and efficiently. However, voltage violations may occurs within defined VVC operation defined time due to various reasons such as sudden variation of generation/load. In order to resolve this issue, local control algorithm has been performed at every 15 minutes (if necessary, it can be other time scale also) based on the obtained reactive power of smart inverter ($Q_{i,pv}^{t*}$) and followed by smart inverter Volt/VAr droop characterstics. The pictorial representation of proposed coordinated scheme has been shown in Fig. 4.2.

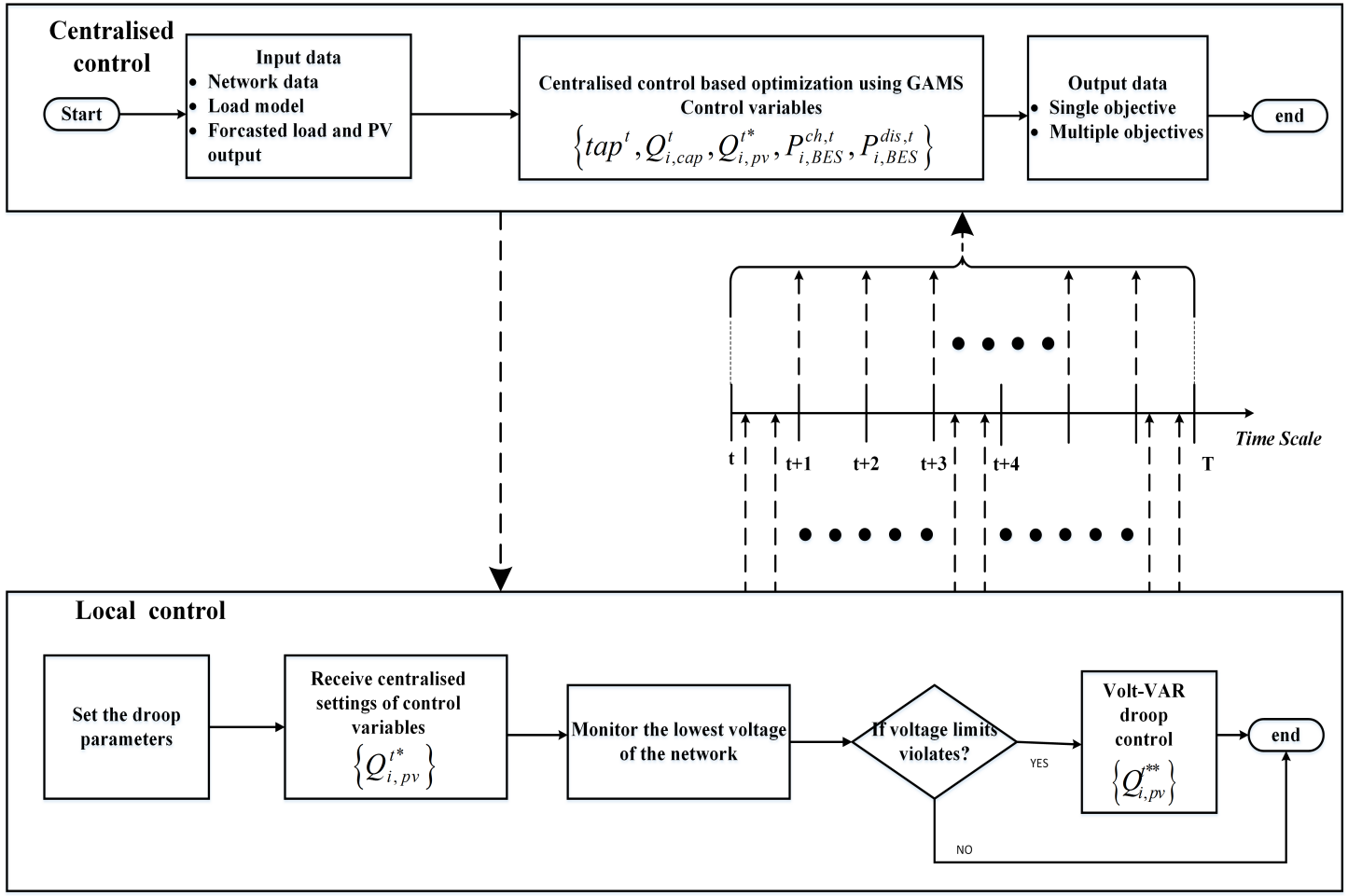

Figure 4.2: Implementation of proposed hierarchical coordinated VVO methodology

4.4.1 Centralised control algorithm

Centralised control algorithm has been performed in two stages as given below

4.4.1.1 Stage 1:

In this stage, the $\varepsilon-$ constraint method has been employed to obtain the set of non-inferior solutions for the objectives OF_1 (minimization of total operating cost) and OF_2 (minimization of voltage deviation). In this method, one objective is considered for the optimization process, while remaining objectives regarded as inequality constraints by considering proper value of parameter $'\varepsilon'$. In the aforementioned problem formulation, OF_1 is considered for the optimization and OF_2 is regarded as inequality constraints as shown below

$$Min.OF_1 \tag{4.21}$$

Subject to operational and system constraints

$$OF_2 \leq \varepsilon \tag{4.22}$$

Equations (4.6) to (4.20) In equation (4.20), OF_2 is constrained by parameter . The value of parameter ε is gradually varies from OF_2 (minimum) to OF_2 (maximum) and the modified objective optimization is solved according the value given to parameter ε and also include operational and system constraints from (4.6) to (4.20). A set of non-inferior solutions can be determined by varying parameter ε from OF_2 (minimum) to OF_2 (maximum), which forms optimal Pareto front of a given multi-objective optimization problem.

4.4.1.2 Stage 2:

In this stage, a fuzzy decision making method has been adopted to obtain the best compromise solution among the set of non-inferior solution. In this method, all the given objective functions are fuzzified and scaled in the range from 0 to 1 by using the linear membership as shown in equation (4.23).

$$\mu(OF_i) = \begin{cases} 1 & ;OF_i \leq OF_i^{\min} \\ \frac{OF_i^{\max} - OF_i}{OF_i^{\max} - OF_i^{\min}} & ;OF_i^{\min} < OF_i < OF_i^{\max} \\ 0 & ;OF_i \geq OF_i^{\max} \end{cases} \tag{4.23}$$

Where membership value of is 1, indicates full compatibility with the sets, while membership value 0, indicates incompatibility. OF_i (maximum) and OF_i (minimum) are the maximum and minimum value of i^{th} objective function. For each of non-inferior solutions, the membership function can be normalized as follows:

$$\mu_D^k = \frac{\left[\sum_{i=1}^{M} \mu(OF_i^k)\right]}{\left[\sum_{k=1}^{K}\sum_{i=1}^{M} \mu(OF_i^k)\right]} \tag{4.24}$$

Where M is the number of objective functions, K is the number of non inferior solutions. Maximum membership value of $\mu(OF_i)$ is treated as best compromise solution.

4.4.2 Local control algorithm

Local control algorithm has been performed based on the setting obtained by the centralised algorithm under hourly basis and volt−var (VV) droop characteristics of PV smart inverter (PVSI). The VV droop characteristics used in this present study has been shown in Fig. 4.3. It is piecewise linear to the voltage and having the four points (A_1, A_2, A_3 and A_4). Before point A_1 , inverter can inject the available maximum reactive power to the point of connection (POC). From point A_1 to A_2, inverter can inject the additional reactive power to the POC. The range between point A_2 and A_3 defined as dead band (DB) range where inverter neither injects nor absorbs reactive power. From point A_3 to A_4, inverter absorbs additional reactive power from the POC. After point A_4, inverter absorbs the available maximum reactive power from the POC. The compensated reactive power ($Q_{i,pv}^{t**}$) at any instant, t is determined using (4.25.

$$Q_{i,pv}^{t**} = \begin{cases} Q_{i,pv}^{\max} & V_i^t < V_1^{A_1} \\ Q_{i,pv}^{t*} + \frac{V - V_2^{A_2}}{V_1^{A_1} - V_2^{A_2}} \left(Q_{i,pv}^{\max} - Q_{i,pv}^{t}\right) & V_1^{A_1} \leq V_i^t < V_2^{A_2} \\ Q_{i,pv}^{t*} & V_2^{A_2} \leq V_i^t \leq V_3^{A_3} \\ -Q_{i,pv}^{t*} - \frac{V - V_3^{A_3}}{V_4^{A_4} - V_3^{A_3}} \left(Q_{i,pv}^{\max} - Q_{i,pv}^{t}\right) & V_3^{A_3} < V_i^t \leq V_4^{A_4} \\ -Q_{i,pv}^{\max} & V_i^t > V_4^{A_4} \end{cases} \tag{4.25}$$

Where, $Q_{i,pv}^{t*}$ is the optimal VAR value obtained by centralised control algorithm. Local control algorithm 4 has been described in algorithm as under, in order to mitigate the voltage violation during cloud movements

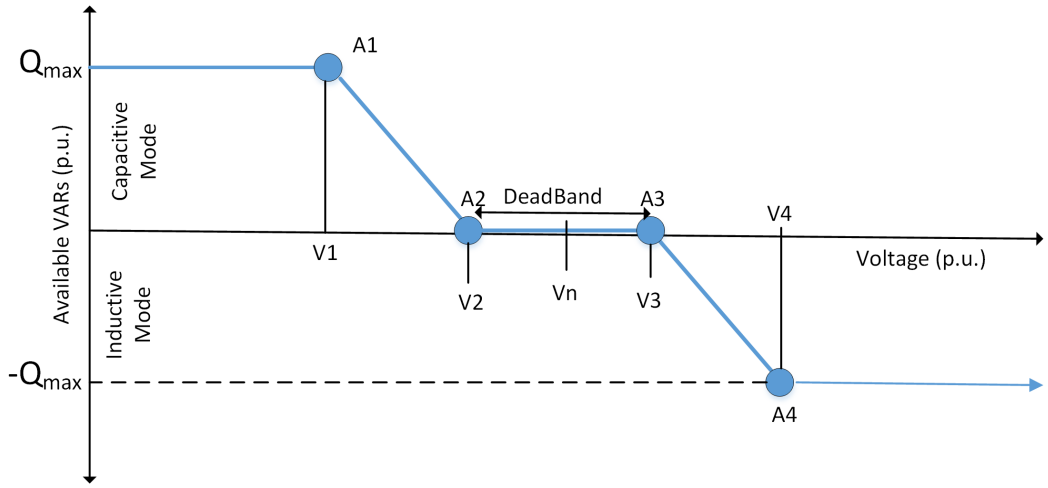

Figure 4.3: Volt VAr droop characteristics of smart inverter

Algorithm 5 Local control algorithm

1: **Input**: feed the settings of traditional and advanced VVC devices as obtained in centralised algorithm. Set the droop controller parameters (A_1, A_2, A_3 and A_4)
2: monitor the lowest voltage of the network, then verify the monitored voltage limits
3: **if** $V_2^{A_2} \leq V_i^t \leq V_3^{A_3}$ **then**
4: PVSI droop controller operates in dead band region. Remain the reactive power dispatch of PVSI same as determined in centralised algorithm
5: **else if** $V_i^t < V_2^{A_2}$ **then**
6: PVSI droop controller operates in capacitive region.
7: PVSI injects the reactive power as governed by (4.25)
8: **else**$V_i^t > V_3^{A_3}$
9: PVSI droop controller operates in inductive region.
10: PVSI absorbs the reactive power as governed by (4.25)
11: **end if**
12: **Output**: Desired additional reactive power compensation has been achieved

4.5 Simulation Results and Discussions

The proposed hierarchical coordinated VVO scheme has been implemented on MATLAB-GAMS environment. GAMS and MATLAB interfacing has been utilised to solve the given problem. Detailed explanation interfacing GAMS and MATLAB has been given in [144]. Optimization of formulated problem has been solved by DICOPT [134], a mixed integer non-linear programming solver of GAMS. The performance of the control scheme has been tested on 33 bus distribution system. The detailed line data and load data of 33 bus system has been taken from [131]. The original system does not have any control devices such as OLTC, SCBs, and PV smart inverter. In order to implement the proposed scheme, some modifications in the original test system have been done to accommodate aforementioned control devices explained as under In modified test system, it is assumed that OLTC transformer is connected between substation and node 1. The OLTC transformer in both distribution systems, can vary the substation secondary side voltage in the range of with 16 tap positions (-8,-7,,-1,0,1,2,,7,8). The change in each step would be 0.625%. Parameters of both modified test systems have been depicted in table 4.1. Further, single line diagram of modified 33 bus distribution system has been shown in Fig. 4.4.

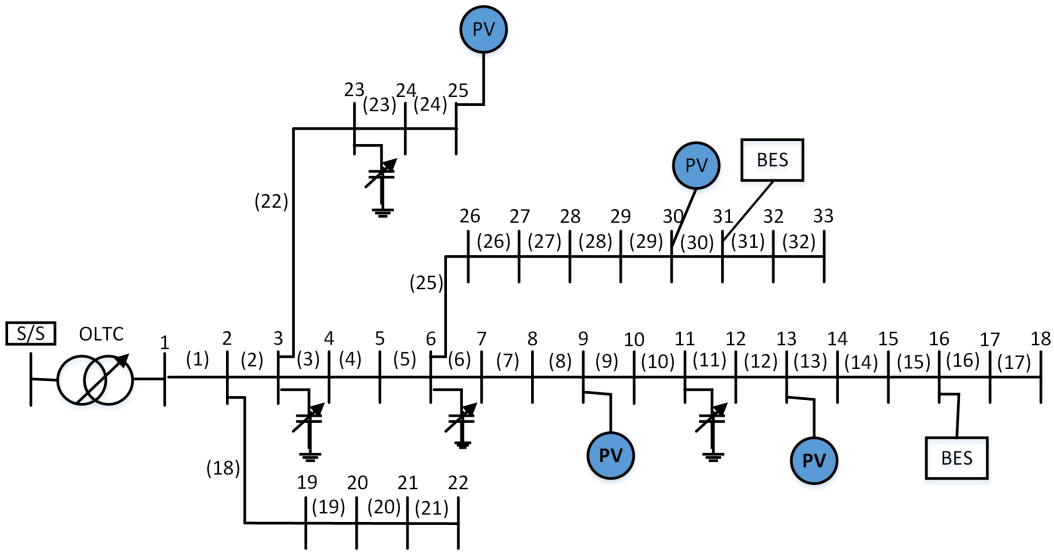

Figure 4.4: Modified 33 bus distribution system

Table 4.2 shows active and reactive power exponents of different types of customers such as industrial, residential and commercial respectively [145].

Load profile, active energy price purchased from grid and PV generation output over

Table 4.1: modified 33 bus distribution system information

Parameters	Test system
Nominal voltage (kV)	12.66
Nominal active power consumption (MW)	3.715
Nominal reactive power consumption (MVAR)	2.3
SCBs installed locations	3,6,11,23
Each SCB capacity (kVAR)	150
PV installed locations	9,13,25,30
Each PV capacity (kVA)	500
BES installed locations	16, 31
Industrial loads	1-3,19-25
Residential loads	4-18
Commercial loads	26-33
Permissible voltage limits	0.95-1.05 pu
DG penetration (%)	53.8%

Table 4.2: value of k_p and k_q and their location

Load type	k_p	k_q	Node location on distribution system
Industrial	0.18	6.00	1-4
Residential	1.04	4.19	5-18,29-33
Commercial	1.5	3.15	19-28

24 hours have been plotted in Fig. 4.5.2. Cost of reactive power from grid is taken as \$0.003/kVAR, active energy price purchased from PV is taken as \$0.04/kWh. Switching cost of OLTC tap and SCB are considered as \$1.4/tap and \$0.24/step respectively. Maximum allowable switching operations of OLTC tap and each SCBs steps over a day are limited to 30 and 10 respectively.

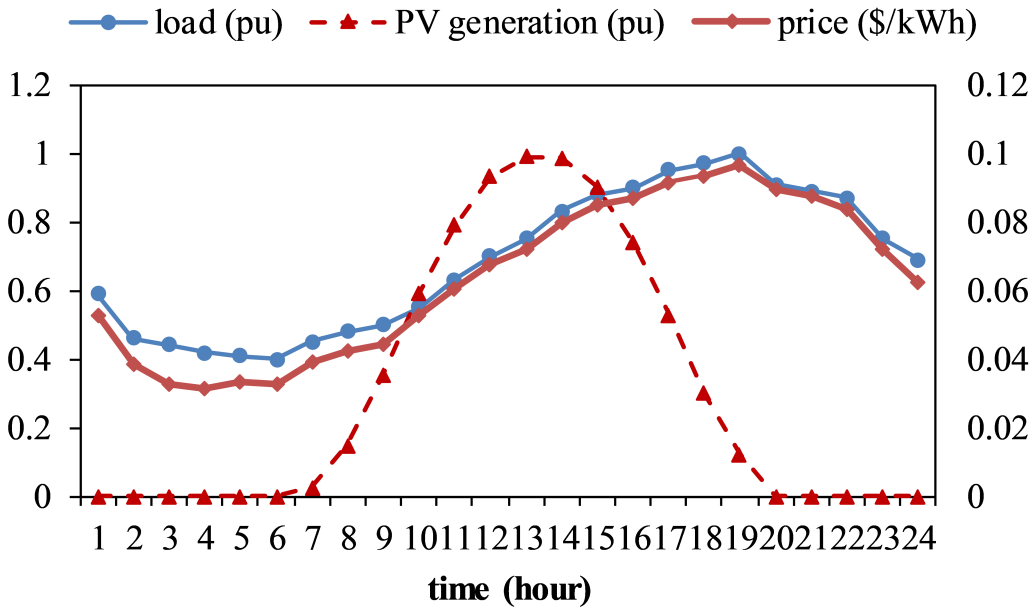

Figure 4.5: Typical load, grid price and PV generation output

4.5.1 Performance of centralised control algorithm considering multi objective

Centralised control algorithm has been performed as described in section 5.1, the constraint method and fuzzy decision method has been employed for the minimization of total operating cost and voltage deviation simultaneously. In order to show that impact of coordinated operation of multiple devices such as OLTC, SCBs, PVSI and BES, five cases has been studied given in Table 4.3.

Table 4.3: Cases studied

cases	Active operation			
	OLTC	SCBS	PVSI	BES
Case 1	✗	✗	✗	✗
Case 2 (method in [36])	✓	✓	✗	✗
Case 3 (proposed method 1)	✓	✓	✓	✗
Case 4 (method in [100])	✓	✓	✗	✓
Case 5 (proposed method 2)	✓	✓	✓	✓

✗- indicates not considered, ✓- indicates considered

4.5.1.1 Case 1: high penetrated PV generation distribution system: no control operation

In this case, OLTC, SCBs, PVSI and BESS are not in active operation. The energy demand of the system has been observed as 74.71 MVAh, in which share of energy consumed and losses are about 72.687 MVAh and 2.023 MVAh respectively. The total operating cost of distribution is calculated as $4115.7. Further, the voltage deviation of the system is noted as 0.69.

4.5.1.2 Case 2: Optimal operation considering traditional VVC devices in high penetrated PV generation distribution system

In this case, OLTC, SCBs are in active operation, where as PVSI and BESS are not in active operation. The pareto front obtained by using constraint method has been plotted in Figure 7 and also shown in Table 4.4 under case 2. It can observed that for OF1 (total operating cost) varies from $3931.59 to $4056.48 and OF2 (voltage deviation) varies from 0.394 to 1.11. The best compromise solution obtained among the set of non-inferior solutions by using fuzzy decision method is solution #3.
The results are depicted in the third column of Table 4.6. From results it is observed that, significant reduction in energy consumption and losses are about 4.22% and 19.92 % compared to case 1 have been obtained respectively. This result in reduction of energy demand about 4.645%. The total operating cost of distribution has been reduced to $3974.81, which results in significant cost savings about $140.89, even after including switching operating cost of OLTC and SCBs. Further, the voltage deviation of the system has been reduced to 0.554.
Thus, coordinated operation of traditional VVC devices (OLTC and SCBs) can efficiently reduce the energy demand up to 4.645% and increase the savings up to $140.89.

4.5.1.3 Case 3: Optimal operation considering both traditional and advanced VVC devices in high penetrated PV generation distribution system

In this case, OLTC, SCBs, PVSI are in active operation, whereas BESS is not active operation. Similarly as case 2, the obtained pareto front optimal solution using constraint method has been plotted in Fig. 4.6. and also shown in Table 4.4 under case 3, where

Table 4.4: Set of non-inferior solutions of the objectives OF1 and OF2 under case 2 and case3

Pareto solutions	Case 2					Case 3				
	OF1	OF2	(OF1)	(OF2)	D	OF1	OF2	(OF1)	(OF2)	D
Solution#1	4056.48	0.394	0	1	0.0805	4006.74	0.211	0	1	0.0823
Solution#2	3991.59	0.4744	0.5196	0.8877	0.1166	3952.3	0.325	0.3757	0.8881	0.104
Solution#3	3974.81	0.554	0.6539	0.7765	0.1167	3924.4	0.439	0.5683	0.7763	0.1106
Solution#4	3962.45	0.633	0.7529	0.6662	0.1134	3905.52	0.553	0.6986	0.6644	0.1122
Solution#5	3954.61	0.713	0.8157	0.5545	0.1091	3890.68	0.667	0.801	0.5525	0.1114
Solution#6	3947.59	0.792	0.8719	0.4441	0.1042	3880.39	0.781	0.872	0.4406	0.108
Solution#7	3942.94	0.872	0.9091	0.3324	0.0989	3873.44	0.895	0.92	0.3288	0.1028
Solution#8	3938.41	0.951	0.9454	0.2221	0.0931	3868.52	1	0.954	0.2257	0.0971
Solution#9	3934.92	1.03	0.9733	0.1117	0.087	3864.63	1.123	0.9808	0.105	0.0894
Solution#10	3931.59	1.11	1	0	0.0805	3861.85	1.23	1	0	0.0823

OF1 varies from \$3861.85 to \$4006.74 and OF2 varies from 0.211 to 1.23 and the best compromise solution obtained by using fuzzy decision method is solution #4. The results are depicted in the fourth column of Table 4.6. From results it is observed that, significant energy consumption and losses reduction about 4.727% and 34.45 % compared to case 1 have been reported respectively. This result in reduction of energy demand about 5.532%. The total operating cost of distribution also has been reduced to \$3905.52, which results in significant cost savings about \$210.18, even after including the smart inverter VAR compensation cost and switching operating cost of OLTC and SCBs. Further, the voltage deviation of the system has been reduced to 0.553.

Thus, association of smart inverter with traditional VVC devices can further reduce the energy demand by 0.887% and increase the cost savings by \$69.29 compared to case 2.

4.5.1.4 Case 4: Optimal operation considering traditional VVC devices in high penetrated PV generation distribution system with BES

In this case, OLTC, SCBs are in active operation, whereas PVSI is not in active operation. In addition, BES operation has been considered. The obtained pareto front optimal solution using constraint method has been plotted in Fig. 4.7 and also shown in Table 4.5 under case 4, where OF1 varies from \$3365.348 to \$3503.442 and OF2 varies from 0.388

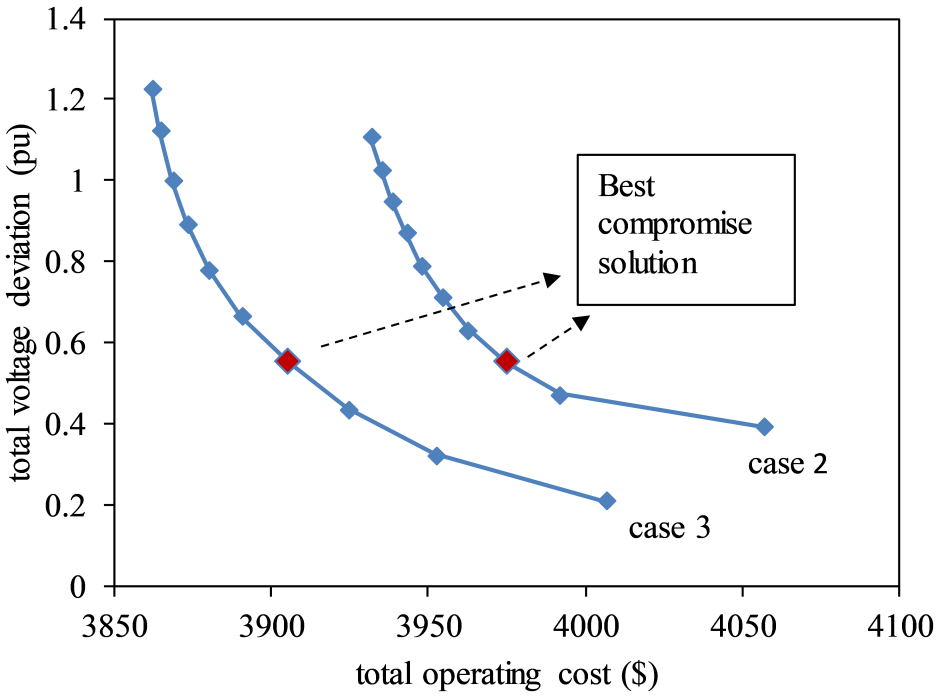

Figure 4.6: Pareto front solution for case 2 and case 3

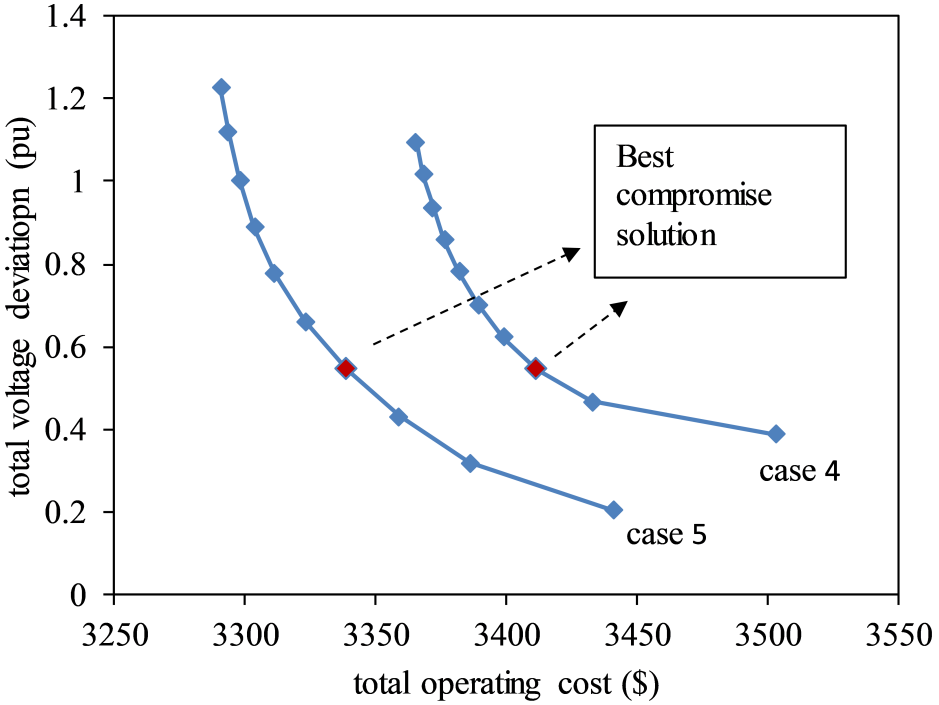

Figure 4.7: Pareto front solution for case 4 and case 5

to 1.094 and the best compromise solution obtained by using fuzzy decision method is solution #3.

The results are depicted in the fourth column of Table 4.6. From results it is observed that, significant energy consumption and losses reduction about 4.756% and 15.47 % compared to case 1 have been reported respectively. This result in reduction of energy demand about 5.032%. The total operating cost of distribution also has been reduced to \$3411.53, which results in remarkable cost savings about \$704.17, even after including the BES operating cost, and switching operating cost of OLTC and SCBs. Further, the voltage deviation of the system has been reduced to 0.545.

In this case, BES operation with traditional VVC devices helps to improve feeder voltage profile, which enhance the voltage reduction range during CVR operation and yields 0.387% more savings in energy demand compared to case 2. Further, optimal energy demand management has been achieved, which results in \$562.83 more savings in total operating cost. The SOC profile of BES has been depicted in Fig. 4.8.

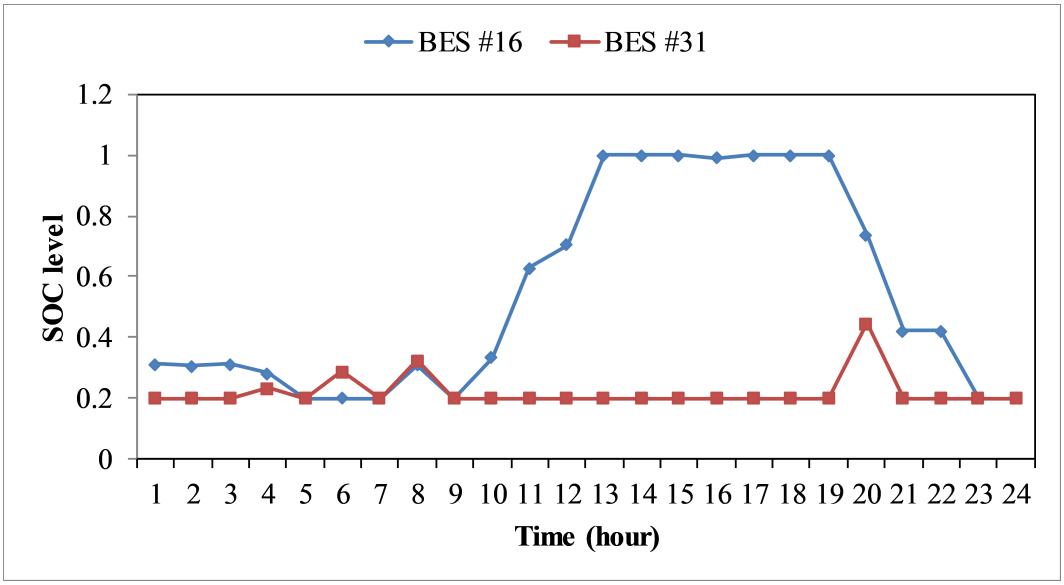

Figure 4.8: SOC profile of BES under case 4

4.5.1.5 Case 5: optimal operation considering both traditional and advanced VVC devices in high penetrated PV generation distribution system with BES

In this case, OLTC, SCBs, and PVSI are in active operation. In addition, optimal BES operation has been considered. The obtained pareto front optimal solution using constraint method has been plotted in Fig. 4.7 and also shown in Table 4.5 under case 5, where OF1 varies from \$3290.7 to \$3441.18 and OF2 varies from 0.204 to 1.225 and the

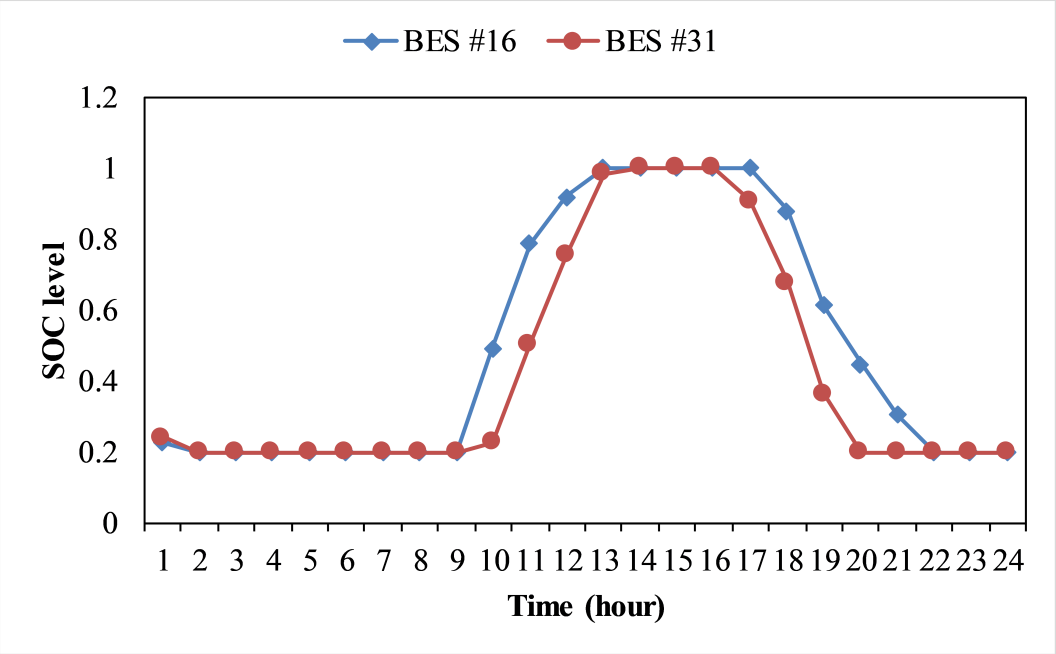

Figure 4.9: SOC profile of BES under case 5

best compromise solution obtained by using fuzzy decision method is solution #4. The results are depicted in the fourth column of Table 4.6. From results it is observed that, significant energy consumption and losses reduction about 5.21% and 39.84 % compared to case 1 have been reported respectively. This result in reduction of energy demand about 6.139%. The total operating cost of distribution also has been reduced to $3338.92, which results in remarkable cost savings about $776.78, even after including the BES operating cost, smart inverter VAR compensation cost and switching operating cost of OLTC and SCBs. Further, the voltage deviation of the system has been reduced to 0.546. In this case, BES operation with traditional and advanced VVC devices helps to improve feeder voltage profile, which enhance the voltage reduction range during CVR operation and yields 1.107% more savings in energy demand compared to case 4. Further, optimal energy demand management has been achieved, which results in $72.61 more cost savings compared to case 4. The SOC profile of BES has been depicted in Fig. 4.9.

4.5.1.6 Impact on losses, voltage profile and VVC devices under different cases:

Active and reactive power losses of the system for five different cases have been plotted in Fig. 4.10 and Fig. 4.11 respectively. From figures it can observed that, among all cases, case 5 has achieved maximum power loss reduction. This shows the effectiveness of the

Table 4.5: set of non-inferior solutions of the objectives OF1 and OF2 under case 4 and case 5

Pareto solutions	Case 4					Case 5				
	OF1	OF2	(OF1)	(OF2)	D	OF1	OF2	(OF1)	(OF2)	D
Solution#1	3503.442	0.388	0	1	0.0801	3441.18	0.204	0	1	0.0829
Solution#2	3432.799	0.466679	0.5116	0.8886	0.1121	3386.14	0.318	0.3658	0.8883	0.104
Solution#3	3411.536	0.545115	0.6655	0.7775	0.1156	3359.05	0.432	0.5458	0.7767	0.1097
Solution#4	3399.006	0.623552	0.7563	0.6664	0.1139	3338.92	0.546	0.6796	0.665	0.1115
Solution#5	3389.363	0.701988	0.8261	0.5554	0.1106	3322.94	0.66	0.7858	0.5534	0.111
Solution#6	3382.124	0.780425	0.8785	0.4443	0.1059	3311.32	0.775	0.863	0.4407	0.1081
Solution#7	3376.511	0.858861	0.9192	0.3332	0.1003	3303.62	0.889	0.9141	0.3291	0.1031
Solution#8	3372.067	0.937298	0.9513	0.2221	0.094	3298.15	1.003	0.9505	0.2174	0.0968
Solution#9	3368.256	1.015734	0.9789	0.1111	0.0873	3293.65	1.118	0.9804	0.1048	0.09
Solution#10	3365.348	1.094171	1	0	0.0801	3290.7	1.225	1	0	0.0829

Table 4.6: Results of three different cases of 33 bus system

parameters	Case 1	Case 2	Case 3	Case 4	Case 5
Energy demand (MVAh)	74.71	71.239	70.577	70.95	70.123
Reduction in Energy demand (%)	—-	4.645	5.532	5.032	6.139
Energy consumption (MVAh)	72.687	69.619	69.251	69.23	68.90
Reduction in Energy consumption (%)	—-	4.22	4.727	4.756	5.21
Energy losses (MVAh)	2.023	1.62	1.326	1.71	1.217
Reduction in Energy losses (%)	—-	19.92	34.45	15.47	39.84
Total voltage deviation	0.69	0.556	0.553	0.545	0.6
Minimum voltage (pu)	0.952	0.95	0.95	0.95	0.95
Maximum voltage (pu)	1.0375	1.028	1.013	1.011	1.006
Cost of energy purchased from grid as well as DG ($)	4115.7	3957.05	3863.82	3392.76	3302.44
Smart inverter VAR compensation cost ($)	—	—-	21.54	——	20.13
Switching operating cost ($)	—-	17.76	20.16	16.36	14.64
BES operating cost ($)	——	——	——	2.415	1.710
Total cost operating cost ($)	4115.7	3974.81	3905.52	3411.53	3338.92
Cost of energy savings ($)	——	140.89	210.18	704.17	776.78

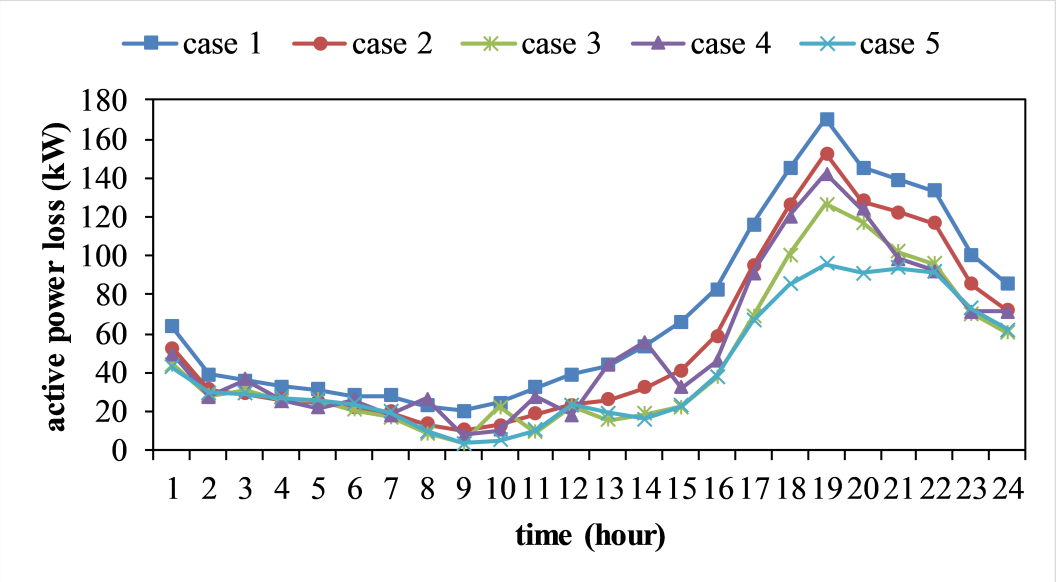

Figure 4.10: Active power loss of the system for different cases

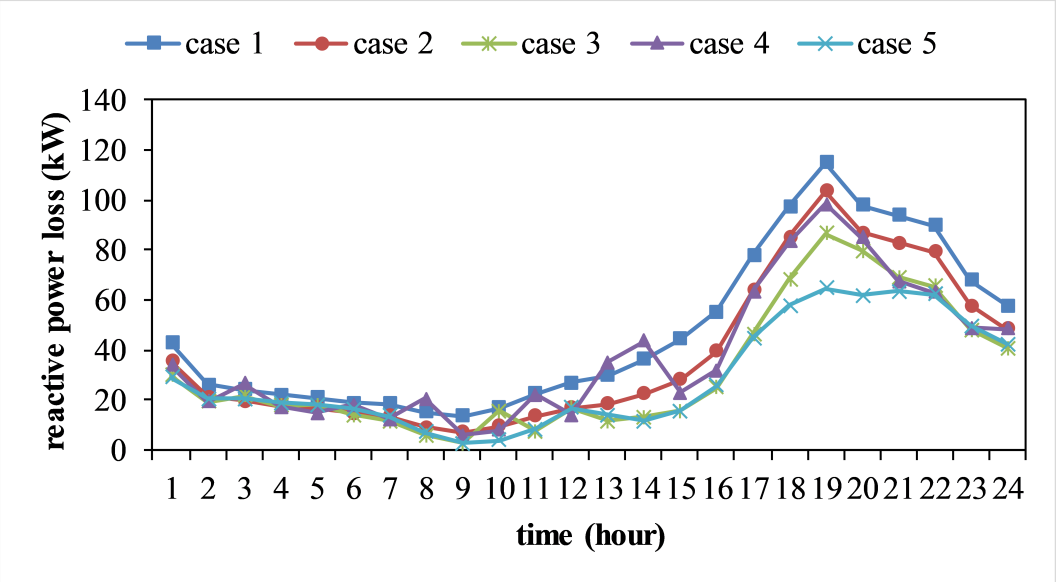

Figure 4.11: Reactive power loss of the system for different cases

optimal coordinated operation of multiple devices such as OLTC, SCBs, smart inverter and BES.

The peak loads of test system are observed at 19th hour, which can be seen from Fig. 4.5.2. The voltage behaviour of the system for different cases at 19th hour has been plotted in Fig. 4.12. Active operation of multiple devices helps to increase the voltage profile as seen in respective cases, which enhance the voltage reduction range along the feeder, thus allows the OLTC to tap down the voltage at the substation. Fig. 4.13 shows

the OLTC tap variations over 24 hours under different cases. Similarly, Fig. 4.14 to Fig. 4.16 shows the status of four SCBs over 24 hours under different cases. It can be observed that, status of capacitor bank kept off in case 3 and case 5 at some hours, which is due to reactive power support provided by smart inverter. Fig. 4.17 and Fig. 4.18 show the optimal reactive power dispatch from PVs smart inverters under case 3 and case 5 respectively. These figures reveal that need of reactive power is much higher in peak loading hours. Further, the reactive power dispatches from smart inverters reduces the VAR burden on capacitors. It can be said that smart inverter may be limit the use of capacitor banks and emerges as future potential candidate for VAR support in global and local domain.

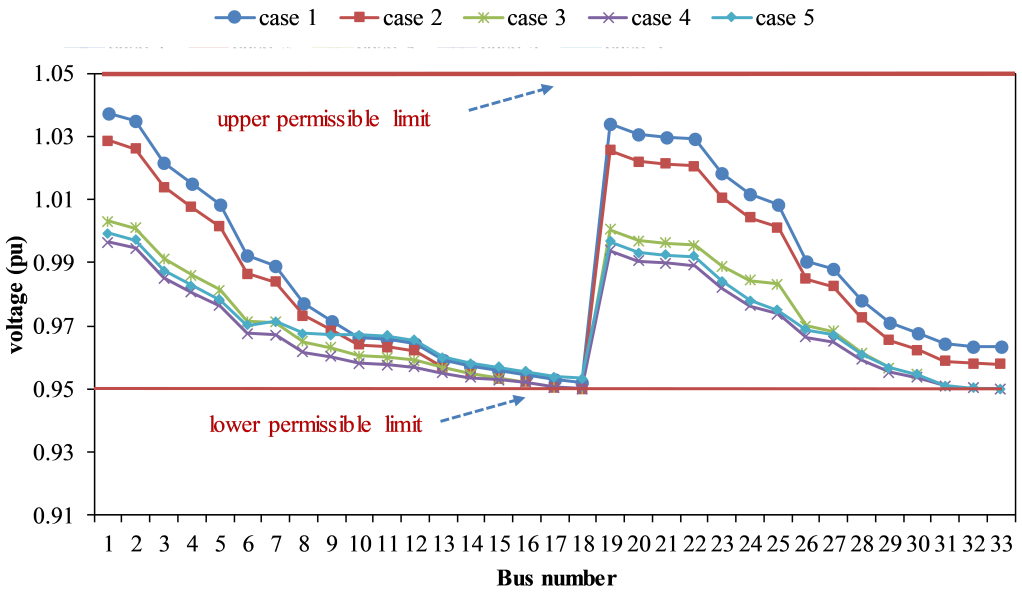

Figure 4.12: Voltage profile of the system at 19th hour

Thus, enhancement of voltage reduction range during CVR operation can be achieved by coordination of multiple voltage control devices and BES.

4.5.1.7 Energy consumption and CVR savings

In this section, the impact of proposed coordinated VVO methodology on energy consumption and CVR savings under different cases has been studied. Fig. 4.19 shows the energy consumption and CVR energy savings under case1 & case 3 over a typical day have been plotted. It can be observed from this figure that, CVR power saving achieved

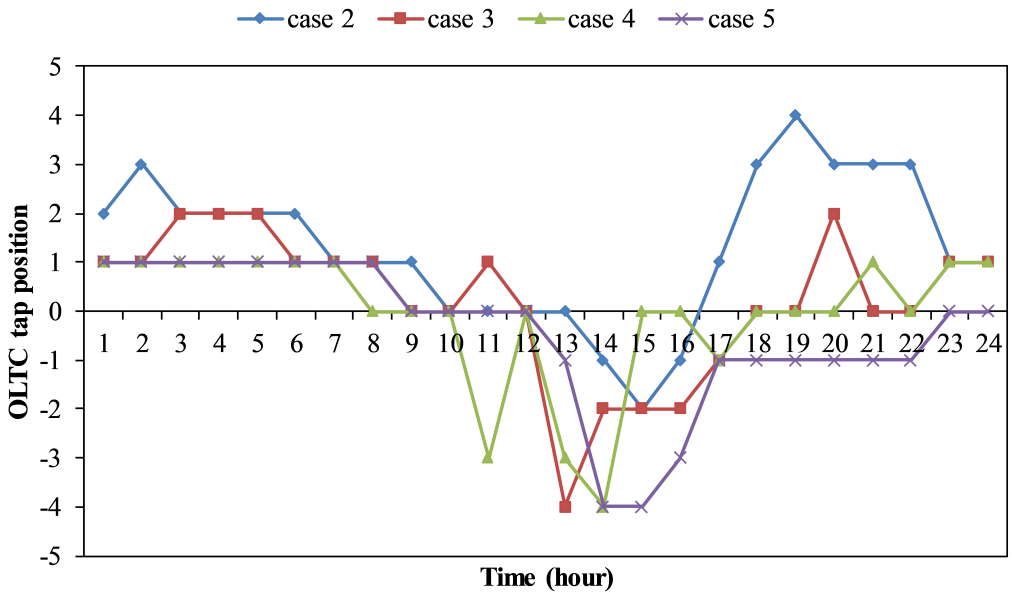

Figure 4.13: OLTC tap variation over a day for different cases

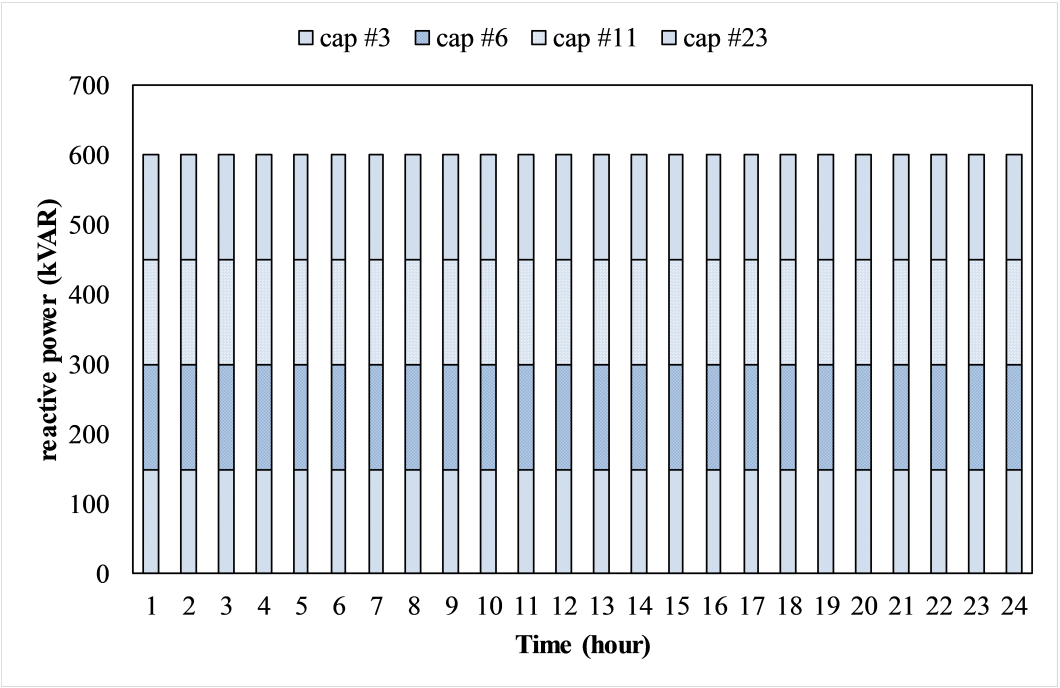

Figure 4.14: status of capacitor banks under case 2 and case 4

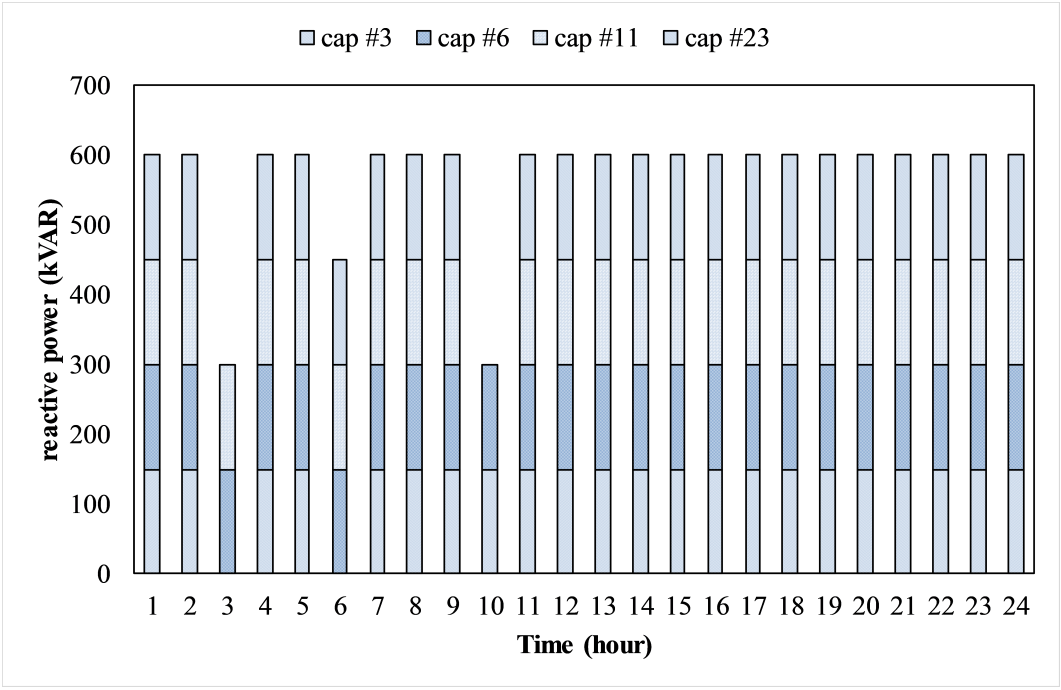

Figure 4.15: status of capacitor banks under case 3

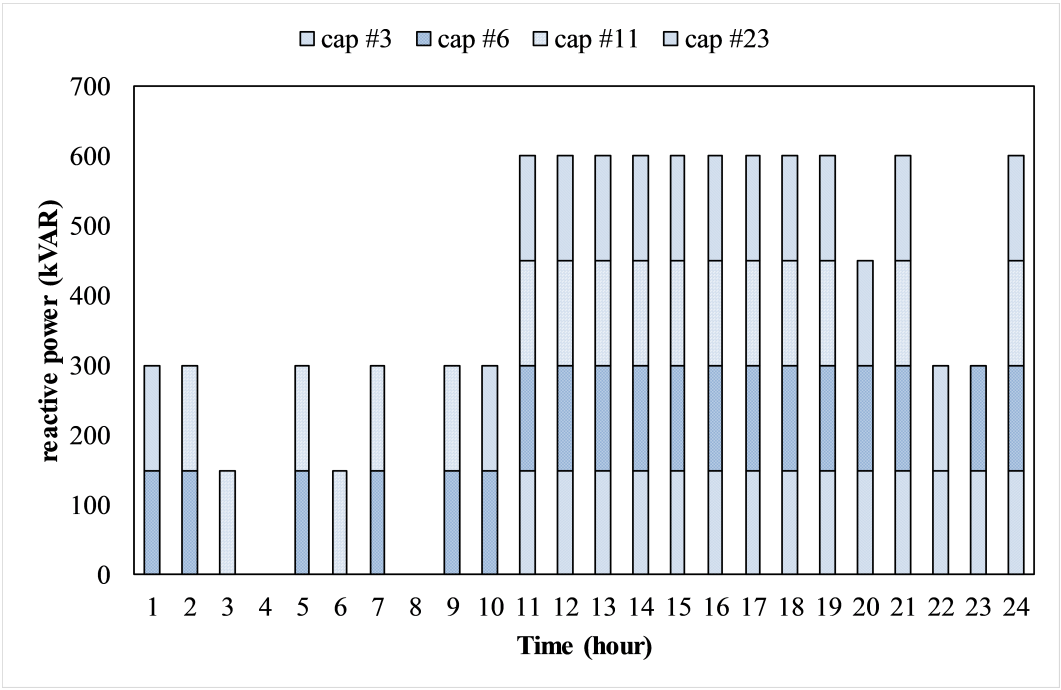

Figure 4.16: status of capacitor banks under case 5

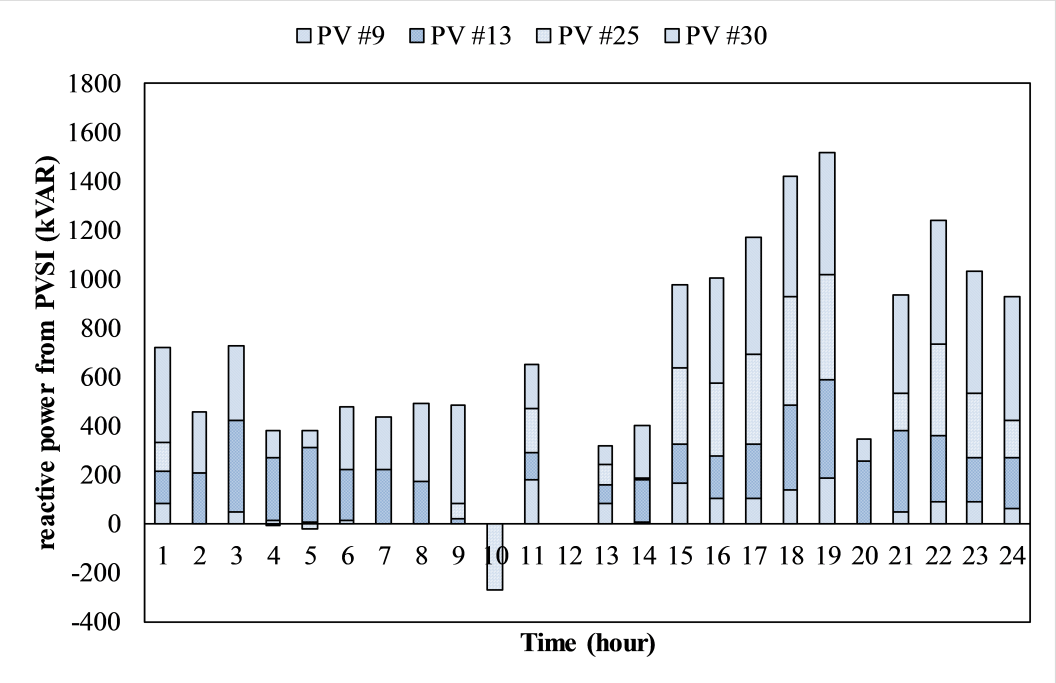

Figure 4.17: Reactive power dispatch of smart inverter under case 3 negative value represents the absorption

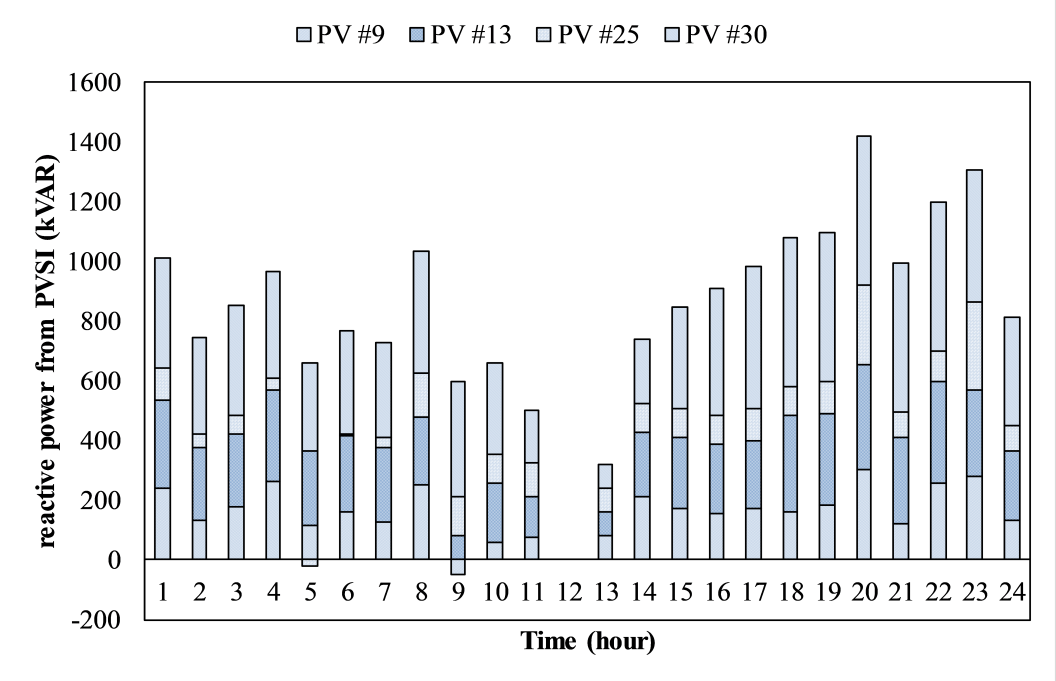

Figure 4.18: reactive power dispatch of smart inverter under case 5 negative value represents the absorption

more at peak loading hours compared to valley loading hours. On an average a power savings of around 143.17 kVA have been obtained. Similarly analysis has been studied,

with association of BES, the energy consumption and CVR energy savings under case1 & case 5 have been plotted in Fig. 4.20. It can be observed that, on an average a savings of around 157.41 kVA have been obtained.

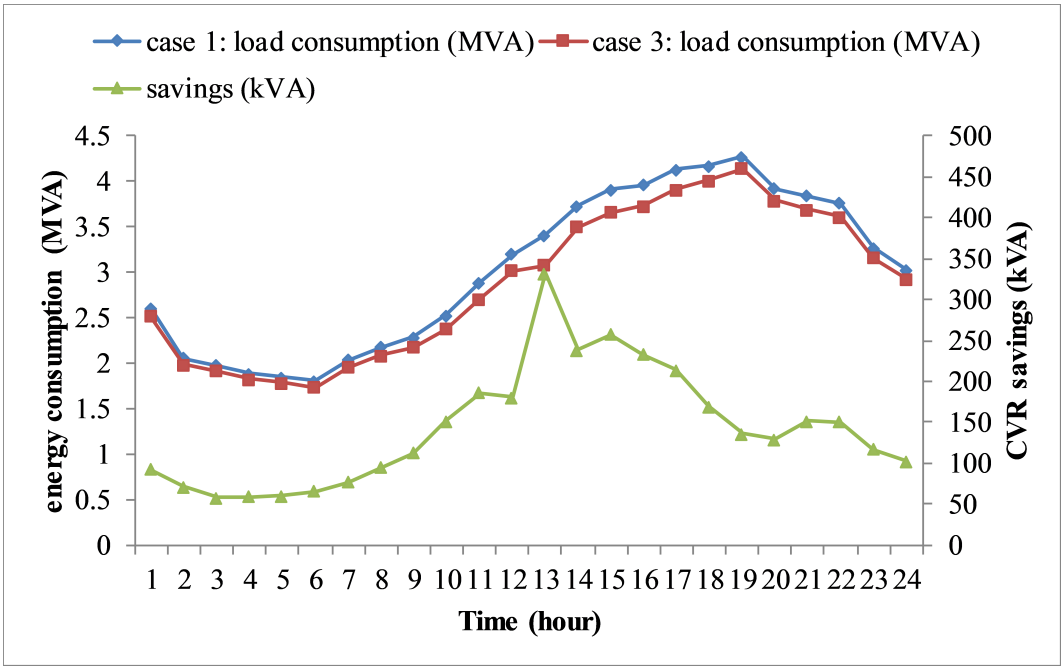

Figure 4.19: Power demand and CVR savings without BES

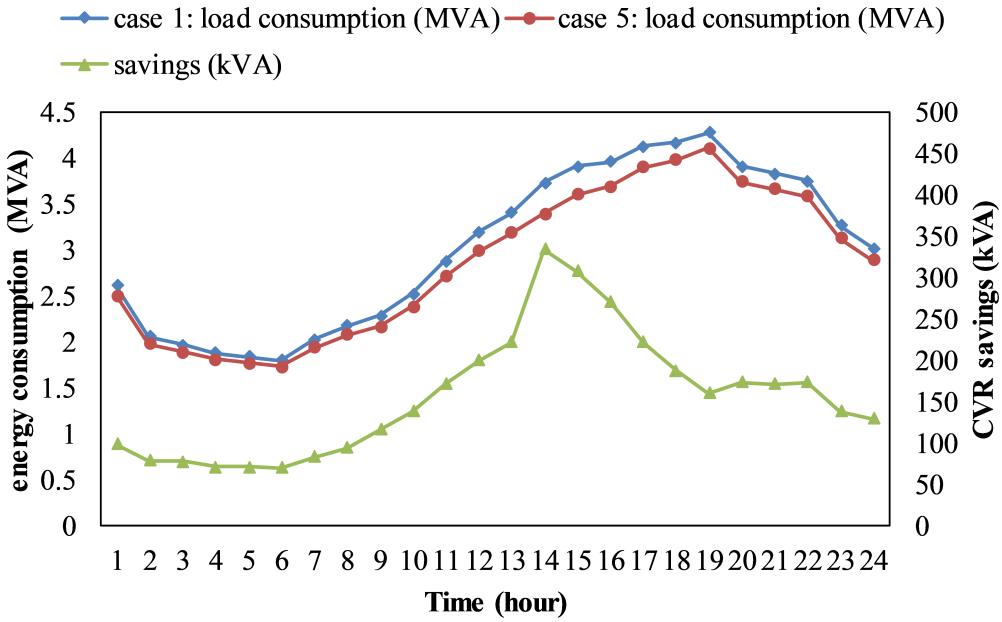

Figure 4.20: Power demand and CVR savings with BES

Thus, it can said that traditional devices with association of smart inverter yields

up to 4.727% reduction in energy consumption. With the incorporation of BES, this reduction can be further increase up to 5.21%

4.5.1.8 Impact on energy demand, consumption and losses

Fig. 4.21 shows total energy demand of the system, in which share of energy consumption and losses has been differentiated under different cases. Among all cases, case 5 achieves minimum energy demand about 70.123 MVAh, in which the amount of energy consumed and losses are about 68.9 MVAh and 1.217 MVAh respectively. Further, Fig. 4.22 shows the cost benefit analysis of different cases. It can be observed that case 1 has maximum operating cost i.e. \$4115.7, whereas case 5 has minimum operating cost i.e. \$3338.92, which results in remarkable savings about \$776.78.

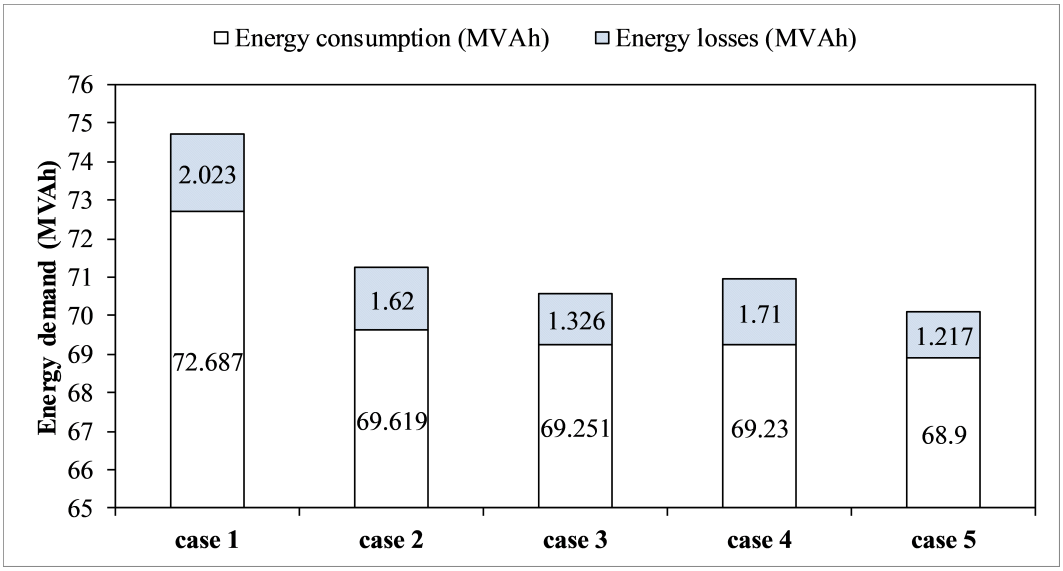

Figure 4.21: Energy demand variation under different cases

4.5.2 Performance of local control algorithm considering cloudy condition

In order to validate the proposed coordinated scheme methodology under fast time scale control, effect of cloud movements has been studied. The typical PV output profile shown in Fig. is valid for a clear sky day. However, in reality many days are fully cloud and partly cloudy days. PV output power fluctuation may exist in the system, when a cloud is passing over the high penetrated PV installed distribution network. For illustration,

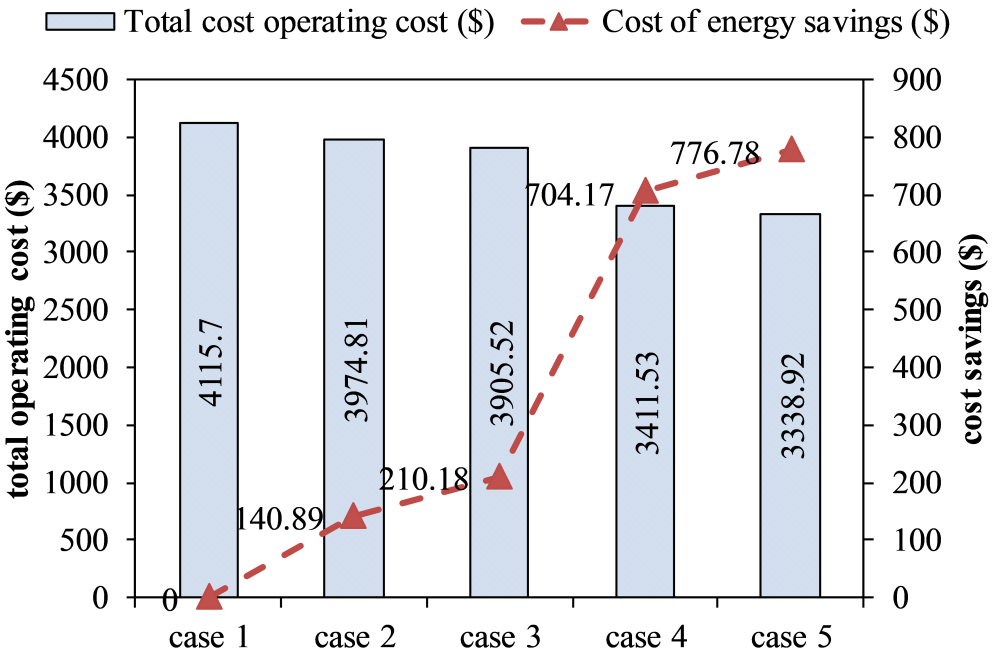

Figure 4.22: Total operating cost and savings under different cases

it is assumed that partly clouds and fully clouds occurred between 13:00 to 14:00 hours for distribution network. During this time span, the forecasted load demand and solar irradiation has been observed as shown in Table 4.7. In this period, the lowest voltage profile at bus 18 and bus 33 becomes more vulnerable to any reduction in PV power generation. In clear cloud day, by using centralised control algorithm, settings of control parameters such as OLTC tap position, SCBs, and smart inverter were obtained and depicted in Table 4.8 during 13:00 to 14:00 hour.

Table 4.7: load and PV output during clear sky, partly and fully cloud day condition

Time (HH:MM)	13:00	13:15	13:30	13:45
Load (pu)	0.75	0.76	0.77	0.78
PV output (pu) @ clear sky	0.9	0.89	0.88	0.87
PV output (pu) @ cloudy sky	0.9	0.667 (25% reduction)	0.44 (50% reduction)	0 (100% reduction)
Aggregated PV output (kW) @ clear sky	1800	1780	1760	1740
Aggregated PV output (kW) @ cloudy sky	1800	1335	880	0

A sudden change in PV generation output assumed and depicted in table 4.6, at

Table 4.8: optimal setting of control devices using centralised control algorithm

Time (HH:MM)	OLTC tap	Aggregated CBs $Q^{t}_{i,cap}$ (kVAR)	Aggregated VAR from PV $Q^{t*}_{i,pv}$(kVAR)	Min. voltage	Aggregated P^{dis}_{BES}(kWh)
13:00 to 14:00	-1	600	320.8	0.95	157

hour 13:15, 13:30, and 13:45, PV output has been reduced by 25%, 50% and 100% from the normal clear sky condition due to partly cloudy and full cloud condition respectively. Consequently, aggregated PV output power drops from 1800 kW to 0 kW as given in table 4.6. The local control algorithm has been utilised as discussed in algorithm 1. The droop parameter setting is given in Appendix A.2. Under the circumstances of cloudy sky, at hour 13:00, lowest voltage of the system is at 0.9502 pu, which is in dead band range of PV smart inverter (PVSI) droop characteristics. At this time instant, PVSI neither inject nor absorbs the additional reactive power. Therefore, reactive power of PVSI at this instant is same as their previous settings (as determined in normal clear day). Under the partly and cloudy days, lowest voltage of the system fall below the lower permissible limit (i.e. 0.95 pu) from hour 13:15 to 13:45, which can be seen in Fig. 4.23. This is due to reduction of PV active power output under cloudy condition. In time duration 13:15 to 13:45 hours, PVSI can provide the additional reactive power support, since the active power output is less than rated capacity of the PVSI. From 13:15 to 13:45 hour, with the support of available reactive power of PVSI as governed by (25), the lowest voltage of the system brought to above lower permissible limit (i.e. 0.95 pu). Subsequently power losses have been reduced as seen in Fig. 4.24. However, energy consumption of system has been increased due to increase in voltages as seen in Fig. 4.25.

The sudden disappearance of cloud or reduction in load demand may result in voltage rise problem. In this situation, the voltage rise can be controlled by absorbing the reactive power through PVSI based on droop controller. In case voltage is still violating the permissible limit, after full utilization of PVSI. The operator has to be reschedule settings of the both traditional and advanced VVC devices. Thus the proposed local control algorithm can efficiently work even in sudden change in the PV power generation.

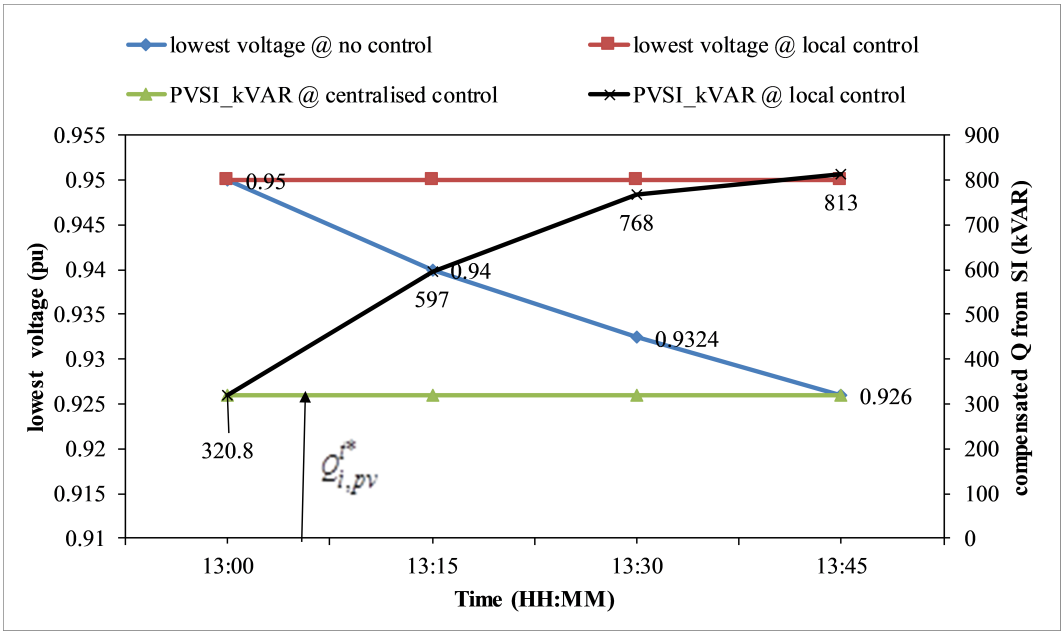

Figure 4.23: Lowest voltage and compensated reactive power from SI during 13:00 to 13:45 hour

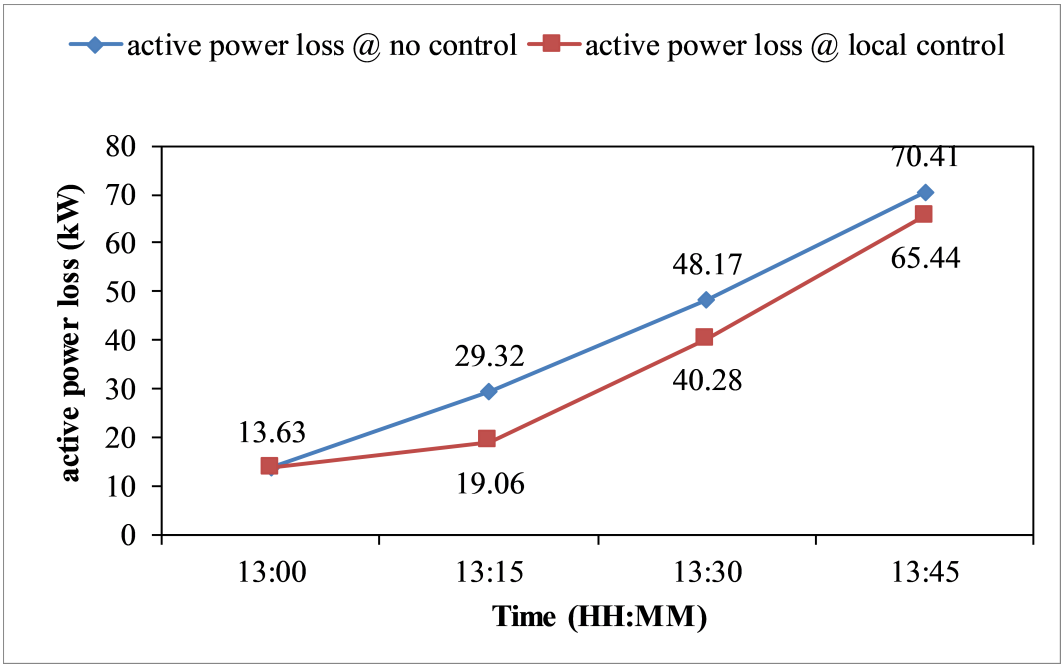

Figure 4.24: Network active power loss during 13:00 to 13:45 hour

4.5.3 Impact of forecast error

In reality, the PV generation output and load of the any particular day have some forecasting error. A stochastic analysis is applied in order to consider the impact of forecast error on results of the optimization problem. Here, the standard deviation of the fore-

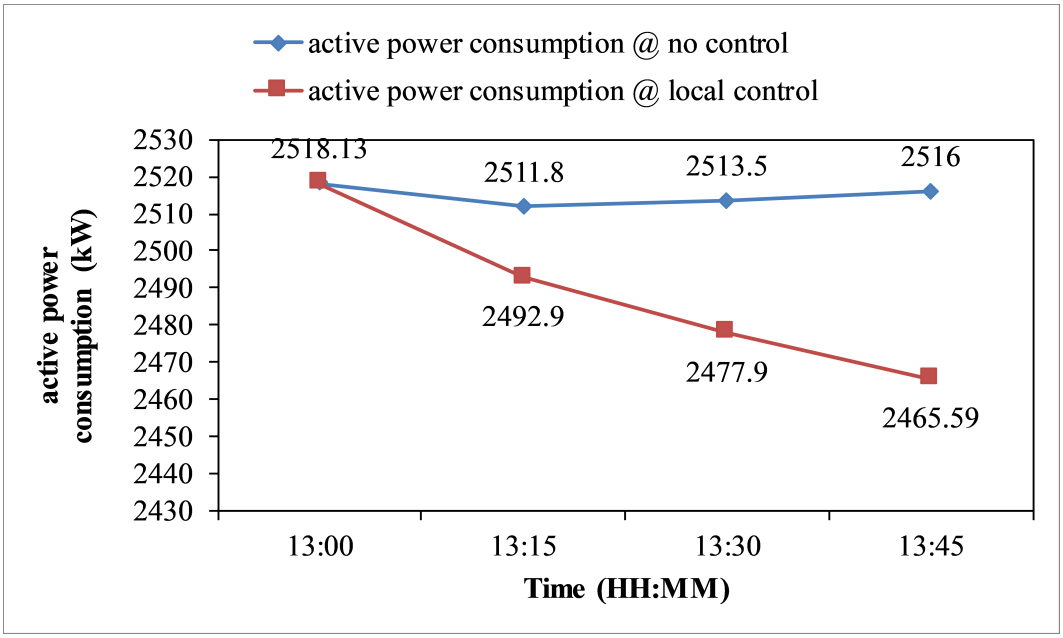

Figure 4.25: Active power consumption during 13:00 to 13:45 hour

casted PV output and load are taken as 15% and 10% of their mean value respectively for each hour. A Gaussian distribution [44] has been employed to simulate the PV output and the load demand, respectively. Further, Monte Carlo simulation has been performed with 500 scenarios. In order to reduce the computational burden, scenarios have been reducing to 15 scenarios by using k-means clustering [137]. The total operating cost and voltage deviation at each hour with/without optimal scheduling of control devices and with/without consideration of forecasted errors have been plotted in the Fig. 4.26 and Fig. 4.27 respectively.

The star symbols ($*$) in Fig. 4.26 indicates the total operating cost value at each hour obtained without consideration of forecasted error (i.e. exactly same as the forecasted values given in Fig. 4.5.2). Similarly, star symbols in Fig. 4.27 indicate the voltage deviation value obtained without consideration of forecasted error. Further, in these figures box plot represents the objective function value with considering forecasted errors at each hour. It can be observed that significant reduction in total operating cost and voltage deviation have been achieved by optimal control setting obtained by case 5 (i.e. proposed scheme) compare to case 1 (i.e. no control) even in consideration of forecast errors. Thus, it can be concluded that the control setting obtained by proposed scheme is effective even in the occurrence of forecast errors.

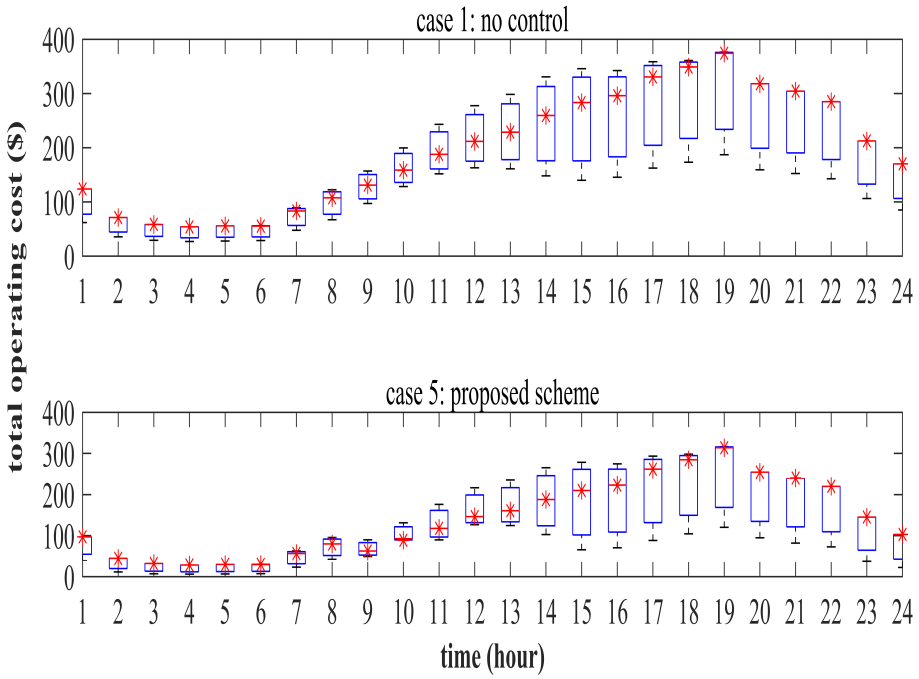

Figure 4.26: Stochastic analysis comparison of total operating cost with/without optimal control & with/without forecasted errors

4.6 Conclusion

This chapter presented an optimally coordinated control scheme for VVC devices and PV smart inverter incorporating BES. In order to do so, a hierarchical coordinated VVO methodology has been developed. The test results demonstrate the significance of the developed scheme in the minimization of voltage regulation, total operating cost and maximization of CVR savings. The major findings reported in this chapter are as follows

- Traditional VVC devices with the association of PV smart inverter yields 0.887% more reduction in energy demand compared to traditional VVC operation.

- BES with the association of PV smart inverter yields 1.107% more reduction in energy demand with enhancing the scope of voltage reduction range in CVR execution.

- Enhancement of voltage reduction range during CVR operation can be achieved by the coordination of multiple voltage control devices and BES.

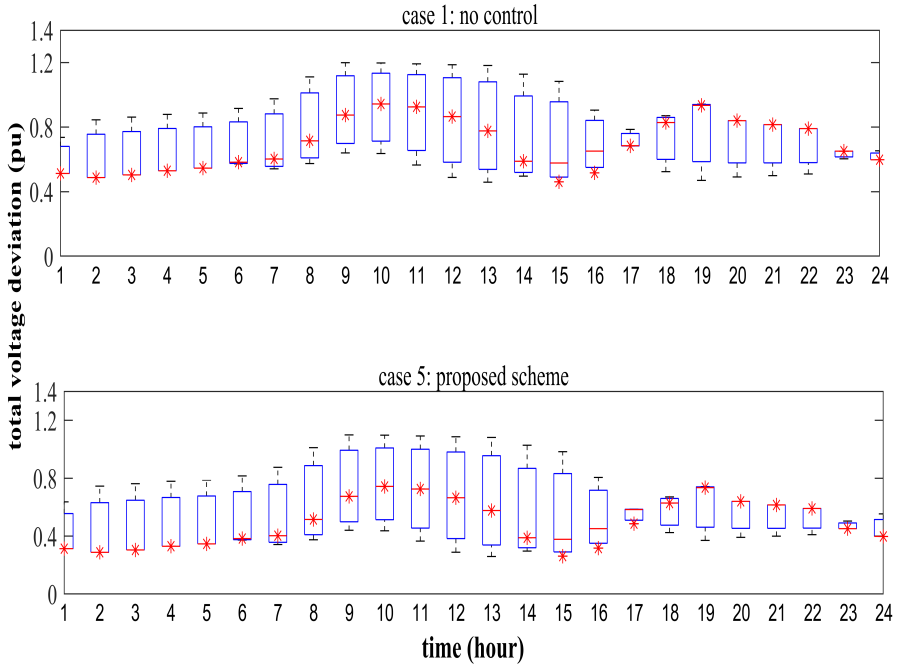

Figure 4.27: Stochastic analysis All node voltage deviation with/without optimal control & with/without forecasted errors

- Proposed scheme achieved reduced switching operating cost of traditional VVC devices and reactive power burden on CB with optimal utilization of smart inverter VAR support.
- The proposed scheme achieved a significant reduction in energy consumption, network losses, total operating costs and voltage deviation.
- The proposed scheme is capable of handling uncertainty and intermittence, such as cloud movements without violating the safe operating voltage limits.